CHARACTERISTICS OF THE MEASUREMENT UNIT OF A FULL-WAVEFORM LASER SYSTEM

B. Jutzi [a], U. Stilla [b]

[a] FGAN-FOM Research Institute for Optronics and Pattern Recognition, 76275 Ettlingen, Germany - jutzi@fom.fgan.de
[b] Photogrammetry and Remote Sensing, Technische Universitaet Muenchen, 80290 Muenchen, Germany - stilla@bv.tum.de

Commission I, WG I/2

KEY WORDS: Accuracy, Analysis, Laser scanning, LIDAR, Measurement, Full-waveform.

ABSTRACT:

The analysis of data derived by full-waveform laser scanning systems is of great interest. In this study, we estimate the impulse response of a laser scanning system capturing the waveform. Considering the impulse response of the system is important for precise waveform analysis. The characteristic of the system has to be mentioned to interpret the pulse properties in an accurate way. We determined by experiments the impulse responses of the laser scanning system for different bandwidths, namely 250 MHz, 750 MHz, 1 GHz, and 6 GHz. By considering the impulse response the measured transmitted waveform of the emitted laser pulse can be adapted. The similarity of the adapted transmitted and received waveform is compared and discussed.

1. INTRODUCTION

The automatic generation of 3-d models for a description of man-made objects, like buildings, is of great interest in photogrammetric research. Laser scanner systems allow a direct and illumination-independent measurement of the range. Laser scanners capture the range of 3-d objects in a fast, contact free and accurate way. Overviews for laser scanning systems are given in (Huising & Pereira, 1998; Wehr & Lohr, 1999; Baltsavias, 1999). A general overview how to develop and design laser systems can be found in textbooks (Jelalian, 1992; Kamermann, 1993).

Current pulsed laser scanner systems for topographic mapping are based on time-of-flight techniques to determine the range of the illuminated object. The elapsed time between the emitted and backscattered laser pulses is typically determined by a threshold detection with analogous electronics. Some systems capture multiple reflections caused by objects which are smaller than the laser beam footprint located in different ranges. Such systems usually record the first and the last backscattered laser pulse.

First pulse as well as last pulse exploitation is used for different applications like urban planning or forestry surveying. While first pulse registration is the optimum choice to measure the hull of partially penetrable objects (e.g. canopy of trees), last pulse registration should be chosen to measure non-penetrable surfaces (e.g. ground surface below vegetation).

Beside the first or last pulse exploitation the complete waveform in between is of interest, because it includes the backscattering characteristic of the illuminated field. Investigations on the waveform analysis were done to explore the vegetation concerning the bio mass, foliage or density (e.g. trees, bushes, and ground). NASA has developed a prototype of the Laser Vegetation Imaging Sensor (LVIS) recording the waveform to determine the vertical density profiles in forests (Blair *et al.*, 1999). This experimental airborne system operates in altitudes up to 10 km and provides a large footprint diameter (up to 80 m) to study different land cover classes.

The spaceborne Geoscience Laser Altimeter System (GLAS) on the Ice, Cloud and Land Elevation Satellite (ICESat) determines changes in range through time, height profiles of clouds and aerosols, ice sheet and land elevations, and vegetation (Brenner *et al.*, 2003; Zwally *et al.*, 2002). It operates with a large footprint diameter (70 m) on Earth and measures elevation changes with decimeter accuracy (Hoften *et al.*, 2000). Table 1 gives an overview of additional specifications.

Beside large footprint systems first developments of small footprint systems were done for monitoring the nearshore bathymetric environments with the Scanning Hydrographic Operational Airborne Lidar Survey system (SHOALS). SHOALS has been in full operation since 1994 (Irish & Lillycrop, 1999; Irish *et al.*, 2000). Recent developments of commercial laser scanner systems led to systems that allow capturing the waveform: RIEGL LMS-Q560, OPTECH ALTM 3100, TOPEYE II. The systems mentioned above are specified to operate with a transmitted pulse width of 5 ns and allow digitization and capturing the waveform with approximately 1 GSample/s. Additional specifications of the small footprint laser systems mentioned above are shown in Table 2.

To interpret the received waveform of the backscattered pulse, a fundamental understanding of the physical background of pulse propagation and surface interaction is important (Jutzi *et al.*, 2002; Wagner *et al.*, 2003). The influence of the surface on the transmitted waveform is discussed by Steinvall (2000) for objects with different shapes taking into account different reflection characteristics. Gardner (1982) and Bufton (1989) investigated the pulse spreading by the impact of the surface structure, e.g. surface slope and vertical roughness within the laser footprint.

The recording of the received waveform offers the possibility to use different methods for the range determination, e.g. peak detection, leading edge detection, average time value detection, constant fraction detection. This topic was investigated by different authors, e.g. Der *et al.*, 1997; Steinvall & Carlsson, 2001; Jutzi & Stilla, 2003; Thiel & Wehr, 2004; Wagner *et al.*, 2004; Vandapel *et al.*, 2004. The analysis of the pulse shape increases the reliability, accuracy, and resolution.

Large footprint laser systems	LVIS	GLAS
Wavelength [nm]	1064	1064
Pulse length at FWHM [a] [ns]	10	6
Pulse repetition rate [Hz]	100-500	40
Laser output energy [mJ]	5	75
Laser beam divergence [mrad]	~5	0.11
Operating altitude [km]	10	600
Scan angle [°]	± 7	0
Detector bandwidth [MHz]	90	0.16 & 1
Digitizer sampling rate [GSamples]	0.5	1

Table 1. Specifications of large footprint laser systems capturing the waveform: LVIS (Blair *et al.*, 1999), and GLAS (Zwally *et al.*, 2002).
[a] Full-width-at-half-maximum

The range estimation is further improved by the comparison between the transmitted and the received waveform. This can be done by signal processing methods (e.g. cross-correlation, inverse filtering), if the sampling of the waveform is done with a high sampling rate. The maximum of the cross-correlation between the transmitted and received signal estimates the range value with a higher reliability and accuracy than considering the received waveform only (Hofton & Blair, 2001; Jutzi & Stilla, 2005; Thiel *et al.*, 2005).

Beside the range determination further surface features can be studied by waveform analysis, namely *reflectance*, *slope* and *roughness*. This specific surface features have an influence on the *amplitude* and *width* of the received waveform (Brenner *et al.*, 2003; Jutzi & Stilla 2002; Steinvall et al., 2004; Wagner *et al.*, 2006). For a parametric description of the pulse properties a Gaussian decomposition method on the waveform can be used (Hofton *et al.*, 2000; Jutzi & Stilla 2005; Persson *et al.*, 2005; Söderman *et al.*, 2005). Nowadays, waveform analysis is more and more established for remote sensing applications especially in forestry (Hug *et al.*, 2004; Reitberger *et al.*, 2006).

Depending on the application different surfaces have to be analyzed, e.g. for urban objects we have to deal with different elevated objects. In rural environment we have to deal with statistically distributed natural objects. The impact of the scene on the received waveform will be discussed using some standard examples (Figure 1). Different elevated object surfaces within the beam corridor lead to a mixture of different range values. A simple situation is given by a horizontal plane surface which will lead to a small pulse (Figure 1b). A plane which is slanted in relation to the viewing direction shows different range values within the footprint. This range interval which is given by the size of the footprint and the orientation of the plane leads to a spread of the pulse width (Figure 1c). A deformation of the pulse form can also be caused by perpendicularly oriented plane surfaces shifted by a small step

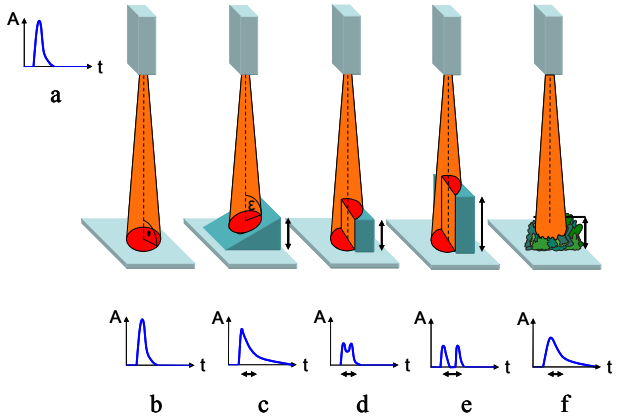

Figure 1. Effects of the surface on the received waveform.
a) transmitted waveform,
b) plane surface,
c) sloped surface,
d) two slightly different elevated areas,
e) two significantly different elevated areas,
f) randomly distributed small objects.

in viewing direction (Figure 1d). A large step leads to two separate pulses (Figure 1e). Several surfaces with different range within the beam can result in multiple pulses. Randomly distributed small objects (e.g. by vegetation) spread over different range values within the beam leads as well to a spread of the pulse width (Figure 1f). These examples show the influence on the waveform by standard surface situations.

Beside the influence of the surface on the waveform the waveform is additionally affected by the used system, especially by the measurement unit itself. For precise waveform analysis it is relevant to consider the system characteristic. This system characteristic can be described by the impulse response of the used laser scanning system. To investigate the impulse response of laser scanning systems experiments are carried out by using receivers with various bandwidths.

In Section 2 an overview on the experimental setup is given. We show a method to estimate the impulse response of the laser scanning system in Section 3. The adaptation of the transmitted waveform by the impulse response and an evaluation for the similarity of the transmitted and received waveform is presented in Section 4. In Section 5 the method is proofed by experiments and results are depicted.

2. EXPERIMENTAL SETUP

An experimental setup was built up for exploring the capabilities of a laser scanning system, which allows capturing the waveform.

Small footprint laser systems	RIEGL LMS-Q560	OPTECH ALTM 3100	TOPEYE II
Wavelength [nm]	1550	1064	1064
Pulse length at FWHM[a] [ns]	4	-	5
Pulse repetition rate [kHz]	Up to 100	50	50
Laser output energy [mJ]	-	-	-
Laser beam divergence [mrad]	≤ 0.5	0.3 or 0.8	1
Operating altitude [m]	< 1500	< 2500	< 1000
Scan angle [°]	± 22.5	± 25	± 20
Detector bandwidth [MHz]	-	-	-
Digitizer sampling rate [GSamples]	1	1	1

Table 2. Specifications of small footprint laser systems capturing the waveform: RIEGL LMS-Q560 (http://www.riegl.com), Optech ALTM 3100 with Intelligent Waveform Digitiser (http://www.optech.on.ca), and TopEye Mark II (http://www.topeye.com).
[a] Full-width-at-half-maximum

2.1 Laser system

The laser system has three main components: an emitter unit, a motion control unit, and receiver unit.

2.1.1 Emitter unit

We use a laser pulse system with a pulse duration of 5 ns at full-width-at-half-maximum (FWHM) and a high repetition rate (42 kHz). The average power of the laser is up to 10 kW. The multi-mode Erbium fiber laser operates at a wavelength of 1550 nm with a beam divergence of 1 mrad. The transmitted waveform of the emitted pulse shows strong random modulation for each emitted pulse. In Figure 2 two examples of the transmitted waveform are depicted. The shape of the waveform depends on the design of the laser system, where the system uses a photodiode to pump the multi mode fiber cavity and a fiber amplifier.

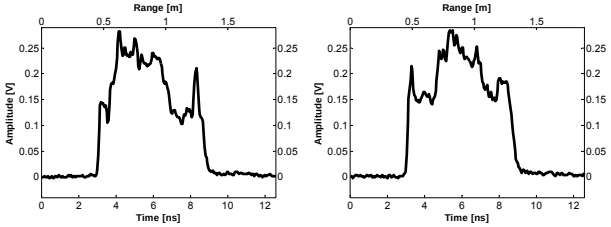

a b

Figure 2. Two samples of the transmitted waveform.

2.1.2 Motion control unit

For the 2-d scanning process a moving mirror is used for an elevation scan with ±15 degrees in vertical direction (320 raster steps) and a rotation stage for an azimuth scan with 360 degree rotation in horizontal direction (variable number and spacing of the raster steps).

2.1.3 Receiver unit

The receiver unit to capture the waveform usually contains PIN [d] or APD [e] photodiodes. For our investigations we used receivers with various bandwidths (250 MHz, 750 MHz, 1 GHz, 7 GHz, and 12 GHz) containing photodiodes sensitive at wavelengths of around 900 to 1700 nm. An overview for the specifications of the receivers which were used in the experiment is given by Table 3. Furthermore, we use an A/D converter with 20 GSamples/s. The A/D conversion and digital recording is accomplished by using a digital memory oscilloscope (Le Croy - Wavemaster 8600A), where the bandwidth of the oscilloscope is limited to 6 GHz.

3. ESTIMATING THE IMPULSE RESPONSE OF THE SYSTEM

The measured received waveform of the backscattered laser pulse depends on the transmitted waveform $s[t]$ of the emitted laser pulse, the impulse response $h_R[t]$ of the measurement unit for the received waveform, the spatial beam distribution of the used laser $P[x,y]$, and the illuminated surface $S[x,y,z]$. The received waveform $r_M[x,y,z,t]$ can be expressed by a convolution of the relevant terms mentioned above and we get

$$r_M[x,y,z,t] = s[t] * h_R[t] * P[x,y] * S[x,y,z] \quad (1)$$

where (*) denotes the convolution operation. The spatial beam distribution is typically Gaussian, and the surface characteristic can be described by its geometry and its reflectance properties (usually a mixture of diffuse and specular). If the transmitted waveform $s[t]$ is as well measured it can be described by

$$s_M[t] = s[t] * h_S[t] , \quad (2)$$

where $h_S[t]$ is the impulse response of the measurement unit of the transmitted waveform. Both impulse responses are mainly affected by the used photodiode(s) and amplifier(s).

Assuming a perfectly flat surface perpendicular to the propagation direction of the laser beam we derive with Equation 1

$$r_M[t] = s[t] * h_R[t] . \quad (3)$$

The measured waveforms $s_M[t]$ and $r_M[t]$ may not necessarily represent the real waveforms of the laser pulses. Depending on the bandwidth of the used photodiodes and amplifiers the waveforms of the used laser system show more or less detailed information. The depicted transmitted waveforms in Figure 2 are recorded with a high bandwidth of 6 GHz and are sampled with 20 GSamples/s. However, we want to characterize the system by its impulse response $h[t]$ independent of the bandwidth of the measurement unit. But, how can we determine the impulse response of the used system?

For estimating the impulse response $h[t]$ of the measurement unit a deconvolution is necessary. The deconvolution can be easily formulated by transforming Eq. 2 and 3 in frequency domain

$$\underline{S}[f] = \frac{\underline{S}_M[f]}{\underline{H}_S[f]} = \frac{\underline{R}_M[f]}{\underline{H}_R[f]} . \quad (4)$$

Terms $\underline{S}[f]$, $\underline{S}_M[f]$, $\underline{R}_M[f]$, $\underline{H}_S[f]$, and $\underline{H}_R[f]$ are the Fourier transforms of the corresponding terms $s[t]$, $s_M[t]$, $r_M[t]$,

Receivers	**TTI-TIA 950** [a]	**TTI-TIA 950** [b]	**New Focus 1611**	**TTI-TIA 4000** [c]	**New Focus 1544** [c]
3dB bandwidth [MHz]	250	750	1000	7000@6000	12000@6000
Detector Material/Type	InGaAs/PIN [d]	InGaAs/PIN	InGaAs/PIN	InGaAs/APD [e]	InGaAs/PIN
Wavelength [nm]	900-1700	900-1700	900-1700	950–1650	950–1650
Minimum NEP [pW/$\sqrt{Hz}$]	3	3	20	16	33
Detector Diameter [µm]	100	100	100	30	25

Table 3. Specifications of the receivers used in the experiment

[a] Gain of 10.0

[b] Gain of 1.0

[c] Bandwidth is limited by the digital oscilloscope to 6 GHz

[d] Positive intrinsic negative diode

[e] Avalanche photodiode

$h_S[t]$, and $h_R[t]$.

This can be written as

$$\underline{R}_M[f] = \underline{S}_M[f] \cdot \frac{\underline{H}_R[f]}{\underline{H}_S[f]} = \underline{S}_M[f] \cdot \underline{H}[f], \quad (5)$$

where $\underline{H}[f]$ is the transfer function of the system.

To estimate the transfer function $\underline{H}[f]$ a frequency-domain division of $\underline{R}_M[f]/\underline{S}_M[f]$ has to be carried out. By the inverse Fourier transformation of $\underline{H}[f]$ we obtain $h[t]$.

Usually the measurement of the transmitted and received waveforms is affected by noise from photodiode and amplifier. Then a straightforward direct division operation leads to a noisy transfer function and as well to a noisy impulse response (Figure 3a) without any significant information.

To avoid this, a sample of N single impulse responses is averaged and we receive the averaged impulse response

$$\overline{h}[t] = \frac{1}{N}\sum_{n=1}^{N} h_n[t], \quad (6)$$

which describes the characteristic of the system. An averaged impulse response (N=1000) is depicted in Figure 3b.

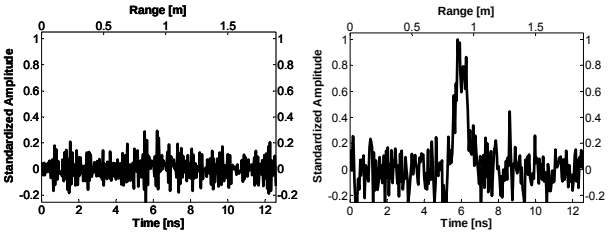

a b

Figure 3. Impulse response of the system:
a) Example of a single impulse response $h_i[t]$,
b) Averaged impulse response $\overline{h}[t]$.

4. ADAPTATION OF THE TRANSMITTED WAVEFORM AND EVALUATION

If the impulse response is determined the transmitted waveform $s_M[t]$ can be adapted to consider the characteristic of the measurement system. Therefore the adaptation of the transmitted waveform is given by

$$s_{\overline{h}}[t] = s_M[t] * \overline{h}[t], \quad (7)$$

where $s_{\overline{h}}[t]$ describes the *adapted transmitted waveform*.

Assuming a perfectly flat surface the shape of the adapted transmitted waveform should be closer to the shape of the received waveform of the backscattered pulse than the transmitted waveform of the emitted pulse. The similarity of the adapted transmitted waveform and the received waveform should be generally increased with this adaptation.

To proof the similarity of the adapted transmitted waveform $s_{\overline{h}}[t]$ and the received waveform $r_M[t]$ the correlation is the favorite method. Therefore the maximum coefficient of the normalized cross-correlation function has to be determined. The normalized cross-correlation function is defined with

$$k'[\tau] = R_{sr}[t+\tau] = \frac{\sum_{t=0}^{M-1} s_{\overline{h}}[t] \cdot r_M[t+\tau]}{\sqrt{\sum_{t=0}^{M-1} s_{\overline{h}}[t]^2 \cdot \sum_{t=0}^{M-1} r_M[t]^2}}, \quad (8)$$

where M is the length of the correlation function $k'[\tau]$ and the maximum correlation coefficient R' is derived by

$$R' = \max(k'[\tau]). \quad (9)$$

To compare the transmitted waveform $s_M[t]$ and the received waveform $r_M[t]$ the correlation coefficient is calculated in the same manner as shown in Equation 8 and 9, where the maximum correlation coefficient is denoted with R. Generally the correlation coefficient is close to 1 for high similarity of the shape of the two waveforms. The result received for R' and R can be compared with each other and evaluated.

5. EXPERIMENTS

To study the impulse response of laser scanning systems experiments are carried out by using receivers with various bandwidths. Figure 4 depicts a schematic description of the processing chain for the experiments.

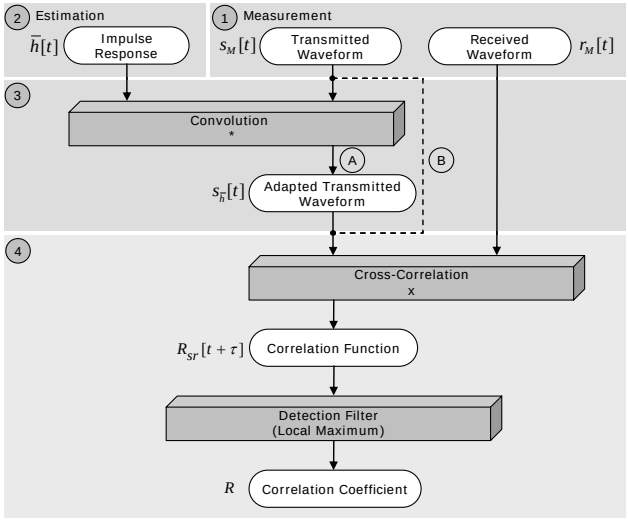

Figure 4. Processing chain.

First the transmitted and the received waveform are measured with the laser scanning system (Figure 4-1) for a sample of N=1000 emitted pulses, where the transmitted and the received waveforms are recorded by separate receivers of the same type and with the same bandwidth.

It has to be mentioned that the receiver TTI-TIA 950 operates at bandwidths of 250 and 750 MHz depending on the pre-selected gain factor, which can be set manually. Furthermore, for the experiments there wasn't an equal pair of receivers with the supported 6 GHz bandwidth of the digital memory oscilloscope available. Therefore we selected two different receivers with a higher bandwidth, where the TTI-TIA 4000 (7 GHz) was used to capture the transmitted waveform and the New Focus 1544 (12 GHz) to capture the received waveform of the laser pulse.

The illuminated target is a flat surface with an orientation perpendicular to the laser beam propagation direction and high material reflectance positioned at a range of approximately 80 m. The high material reflectance is necessary to capture the

Receivers	TTI-TIA 950	TTI-TIA 950	New Focus 1611	TTI-TIA 3000 [a] New Focus 1544 [a]
3dB bandwidth [MHz]	250	750	1000	@6000
Ⓐ Average value $\overline{R}$ of the correlation coefficient	0.9734	0.9756	0.9737	0.9688
Ⓑ Average value $\overline{R}'$ of the correlation coefficient	0.9782	0.9817	0.9776	0.9745
Ⓐ Standard deviation σ_R of the correlation coefficient	0.0085	0.0585	0.0072	0.0321
Ⓑ Standard deviation $\sigma_{R'}$ of the correlation coefficient	0.0075	0.0588	0.0068	0.0320

Table 3. Specifications of the receivers used in the experiment.
[a] Bandwidth is limited by the digital oscilloscope to 6 GHz

waveform with receivers of low sensitivity. Especially the receivers with bandwidths greater than 1 GHz have a very low sensitivity.

To estimate the impulse response of the system (Figure 4-2) the measured sample is processed as described in Section 3. The average of the single impulse responses derived by the various receiver pairs is depicted in Figure 5. Measurements are carried out for the following bandwidths: 250 MHz, 750 MHz, 1 GHz, and 6 GHz. With increasing bandwidth the width of the impulse response decreases. Caused by the small number of the measured samples (N=1000) the estimated impulse response shows still some noise characteristics, especially the impulse responses derived by the receivers with low bandwidths. For further processing only the values greater than zero of the impulse response itself are considered and the background noise is set to zero. Beside this straightforward estimation of the impulse response further investigations in frequency-domain for noise reduction (e.g. low pass filtering) might be of interest for performance optimization, but this was not further investigated in this paper.

However the estimated impulse response is convolved with the transmitted waveform for each emitted pulse to determine the adapted transmitted waveform $s_{\overline{h}}[t]$ (Figure 4-3).

To evaluate the transmitted waveforms $s_M[t]$ and $s_{\overline{h}}[t]$ the correlation coefficient of the transmitted and the received

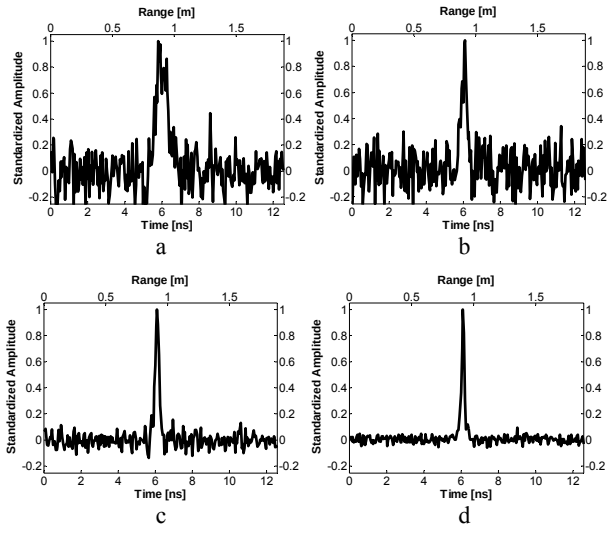

Figure 5. Impulse responses of the laser scanning system for various receivers:
a) 250 MHz bandwidth,
b) 750 MHz bandwidth,
c) 1 GHz bandwidth,
d) 6 GHz bandwidth.

waveform is calculated for each single emitted laser pulse (Figure 4-4). The correlation coefficient is extracted from the correlation function by detecting the local maximum and determines the maximum value. To compare the adapted (Figure 4-A) and the corresponding measured transmitted waveform (Figure 4-B, dashed line), the correlation coefficients are determined and compared with each other. Then the average values $\overline{R}$ ($\overline{R}'$) and the standard deviation values σ_R ($\sigma_{R'}$) of the correlation coefficient R (R') for 1000 samples is calculated for each measurement. The results are presented in Table 3.

For all investigated bandwidths the average value $\overline{R}'$ of the correlation coefficient derived by the adapted transmitted waveform $s_{\overline{h}}[t]$ is higher than the average value $\overline{R}$ derived by the transmitted waveform $s_M[t]$. The standard deviation $\sigma_{R'}$ of the correlation coefficient derived by the adapted transmitted waveform is lower for three of four measurements.

6. DISCUSSION

All experiments are carried out in the same manner, only receivers with various bandwidths are used for each measurement. The similarity of the shape of the transmitted waveform and the received waveform is generally very high, but could be increased with the *adapted transmitted waveform*. It has to be mentioned, that the significance is not as high as we expected. In relation to the amplitude of the estimated impulse response large noise influences could be observed at low bandwidths. With increasing the bandwidth the width of the impulse response decreases. This might depend on the manufacturing accuracy of the used photodiodes. The width of the adapted impulse responses $\overline{h}[t]$ is smaller than the width of the transmitted waveform $s_M[t]$ of the emitted laser pulse (compare Figure 3 and 5). The convolution of the impulse response with the transmitted waveform has a low pass effect on the transmitted waveform.

7. CONCLUSION

In this work it was shown that the waveform is affected by the measurement unit. The influence of the measurement unit on capturing the transmitted and received waveforms of the laser pulse can be described by the impulse response which characterizes the system. To study the measurement unit we determined the impulse response of the laser scanning system for different bandwidths, namely 250 MHz, 750 MHz, 1 GHz, and 6 GHz. Considering the impulse response by calculating the adapted transmitted waveform increases the similarity of the shape of the transmitted and the received waveform. For precise waveform analysis the similarity of both measured waveforms is important to determine the influence of the surface in an accurate way. This is helpful to extract surface features with

high accuracy, e.g. range determination by cross-correlation. The experiments we carried out are general investigations for a laser scanning system which records the full-waveform of laser pulses.

REFERENCES

Baltsavias EP (1999) Airborne laser scanning: existing systems and firms and other resources. ISPRS Journal of Photogrammetry & Remote Sensing 54: 164-198.

Blair JB, Rabine DL, Hofton MA (1999) The Laser Vegetation Imaging Sensor (LVIS): A medium-altitude, digitization-only, airborne laser altimeter for mapping vegetation and topography. ISPRS Journal of Photogrammetry & Remote Sensing 56: 112-122.

Brenner AC, Zwally HJ, Bentley CR, Csatho BM, Harding DJ, Hofton MA, Minster JB, Roberts LA, Saba JL, Thomas RH, Yi D (2003) Geoscience Laser Altimeter System (GLAS) - Derivation of Range and Range Distributions From Laser Pulse Waveform Analysis for Surface Elevations, Roughness, Slope, and Vegetation Heights. Algorithm Theoretical Basis Document - Version 4.1.

Bufton JL (1989) Laser Altimetry Measurements from Aircraft and Spacecraft. Proceedings of the IEEE, Vol. 77, No. 3, 463-477.

Der S, Redman B, Chellappa R (1997) Simulation of error in optical radar measurements. Applied Optics 36 (27), 6869-6874.

Gardner CS (1982) Target signatures for laser altimeters: an analysis. Applied Optics, Volume 21, Issue 3, 448-453.

Hofton MA, Blair JB (2001) Laser altimeter return pulse correlation: A method for detecting surface topographic change. Journal of Geodynamics special issue on laser altimetry 34, 491-502.

Hofton MA, Minster JB, Blair JB (2000) Decomposition of laser altimeter waveforms. IEEE Transactions on Geoscience & Remote Sensing 38 (4), 1989–1996.

Hug C, Ullrich A, Grimm A (2004) LITEMAPPER-5600 - a waveform digitising lidar terrain and vegetation mapping system. International Archives of Photogrammetry, Remote Sensing & Spatial Information Sciences 36, Part 8/W2, 24-29.

Huising EJ, Gomes Pereira LM (1998) Errors and accuracy estimates of laser data acquired by various laser scanning systems for topographic applications. ISPRS Journal of Photogrammetry & Remote Sensing 53: 245-261.

Irish JL, Lillycrop WJ (1999) Scanning laser mapping of the coastal zone: the SHOALS system. ISPRS Journal of Photogrammetry & Remote Sensing 54: 123-129.

Irish JL, McClung JK, and Lillycrop WJ (2000) Airborne lidar bathymetry: the SHOALS system. PIANC Bulletin. 2000 (103): 43-53.

Jelalian AW (1992) Laser Radar systems. Norwood, MA, Boston: Artech House.

Jutzi B, Eberle B, Stilla U (2002) Estimation and measurement of backscattered signals from pulsed laser radar. In: Serpico SB (ed) (2003) Image and Signal Processing for Remote Sensing VIII, SPIE Proc. Vol. 4885: 256-267.

Jutzi B, Stilla U (2003) Laser pulse analysis for reconstruction and classification of urban objects. In: Ebner H, Heipke C, Mayer H, Pakzad K (eds) Photogrammetric Image Analysis PIA'03. International Archives of Photogrammetry & Remote Sensing. Vol. 34, Part 3/W8, 151-156.

Jutzi B, Stilla U (2005) Measuring and processing the waveform of laser pulses. In: Gruen A, Kahmen H (eds) Optical 3-D Measurement Techniques VII. Vol. I, 194-203.

Kamermann GW (1993) Laser Radar. In: Fox CS (ed) Active Electro-Optical Systems, The Infrared & Electro-Optical Systems Handbook. Michigan: SPIE Optical Engineering Press.

Papoulis A (1984) Probability, Random Variables, and Stochastic Processes. Tokyo: McGraw-Hill.

Persson Å, Söderman U, Töpel J, Ahlberg S (2005) Visualization and analysis of full-waveform airborne laser scanner data. In: Vosselman G, Brenner C (Eds) Laser scanning 2005. International Archives of Photogrammetry & Remote Sensing 36, Part 3/W19, 109-114.

Reitberger J, Krzystek P, Heurich M (2006) Full-Waveform analysis of small footprint airborne laser scanning data in the Bavarian forest national park for tree species classification. In: Koukal T, Schneider W (Eds) 3D Remote Sensing in Forestry. 218-227.

Skolnik MI (1980) Introduction to radar systems. McGraw-Hill International Editions, Second Edition.

Söderman U, Persson Å, Töpel J, Ahlberg S (2005) On analysis and visualization of full-waveform airborne laser scanner data. Laser Radar Technology and Applications X. In: Kamerman W (ed) SPIE Proc. Vol. 5791: 184-192.

Steinvall O (2000) Effects of target shape and reflection on laser radar cross sections. Applied Optics 39 (24), 4381-4391.

Steinvall O, Carlsson T (2001) Three-dimensional laser radar modeling. In: Kamerman GW (Ed) Laser Radar Technology and Application VI, SPIE Proc. Vol. 4377, 23-34.

Steinvall O, Larsson H, Gustavsson F, Chevalier T, Persson Å, Klasén L (2004) Characterizing targets and backgrounds for 3D laser radars. Military Remote Sensing. In: Kamerman W, Willetts DV (eds) SPIE Proc. Vol. 5613: 51-66.

Thiel KH, Wehr A (2004) Performance Capabilities of Laser-Scanners - An Overview and Measurement Principle Analysis. International Archives of Photogrammetry, Remote Sensing & Spatial Information Sciences 36, Part 8/W2, 14–18.

Thiel KH, Wehr A, Hug C (2005) A New Algorithm for Processing Fullwave Laser Scanner Data. EARSeL 3D-Remote Sensing Workshop, CDROM.

Vandapel N, Amidi O, Miller JR (2004) Toward Laser Pulse Waveform Analysis for Scene Interpretation. IEEE International Conference on Robotics and Automation (ICRA 2004).

Wagner W, Ullrich A, Briese C (2003) Der Laserstrahl und seine Interaktion mit der Erdoberfläche. Österreichische Zeitschrift für Vermessung & Geoinformation, VGI 4/2003, 223-235.

Wagner W, Ullrich A, Ducic V, Melzer T, Studnicka N (2006) Gaussian Decomposition and Calibration of a Novel Small-Footprint Full-Waveform Digitising Airborne Laser Scanner. ISPRS Journal of Photogrammetry & Remote Sensing, 60 (2), 100-112.

Wagner W, Ullrich A, Melzer T, Briese C, Kraus K (2004) From single-pulse to full-waveform airborne laser scanners: Potential and practical challenges. In: Altan MO (ed) International Archives of Photogrammetry & Remote Sensing. Vol. 35, Part B3, 201-206.

Wehr A, Lohr U (1999) Airborne laser scanning – an introduction and overview. ISPRS Journal of Photogrammetry & Remote Sensing 54: 68-82.

Zwally HJ, Schutz B, Abdalati W, Abshire J, Bentley C, Brenner A, Bufton J, Dezio J, Hancock D, Harding D, Herring T, Minster B, Quinn K, Palm S, Spinhirne J, Thomas R (2002) ICESat's laser measurements of polar ice, atmosphere, ocean, and land. Journal of Geodynamics 34 (3–4), 405–445.